

Document downloaded from the institutional repository of the University of Alcalá: <http://dspace.uah.es/dspace/>

This is a postprint version of the following published document:

Dominguez-Lopez, A., Lopez-Gil, A., Martin-Lopez, S., Gonzalez-Herraez, M., 2014, "Balanced detection in Brillouin optical time domain analysis", Proc. SPIE 9157, 23rd International Conference on Optical Fibre Sensors, 915765.

Available at <http://dx.doi.org/10.1117/12.2059295>

Copyright 2013 Society of Photo Optical Instrumentation Engineers. One print or electronic copy may be made for personal use only. Systematic electronic or print reproduction and distribution, duplication of any material in this paper for a fee or for commercial purposes, or modification of the content of the paper are prohibited

(Article begins on next page)



This work is licensed under a

Creative Commons Attribution-NonCommercial-NoDerivatives
4.0 International License.

Balanced detection in Brillouin optical time domain analysis

Alejandro Dominguez-Lopez*, Alexia Lopez-Gil, Sonia Martin-Lopez, Miguel Gonzalez-Herraez
Dept. of Electronics, University of Alcala. Polytechnic School, 28871 Alcala de Henares, Spain

ABSTRACT

We propose the use of balanced detection in Brillouin Optical Time Domain Analysis (BOTDA) sensors. Balanced detection can be effectively accomplished among the Stokes and anti-Stokes bands in the probe signal. This type of detection leads to a doubling of the trace amplitude and at least a $\sqrt{2}$ increase in signal to noise ratio over the conventional configuration. Moreover, it leads to a complete cancellation of the common-mode noise in the probe signal, including relative intensity noise in Raman-assisted configurations. We show all these benefits both theoretically and experimentally.

Keywords: Brillouin scattering, Raman scattering, distributed optic fiber sensor, balanced detection, temperature sensor.

1. INTRODUCTION

Brillouin-based distributed temperature and strain fiber sensors have become strong competitors of traditional multi-point sensing systems, generating a remarkable interest for several industrial applications. Specifically, Brillouin Optical Time Domain Analysis (BOTDA) systems are increasingly used in monitoring large civil structures, such as dams, electrical grids, bridges, railways, etc. Of course, a huge research effort is invested on extending the measuring range of these sensors. In order to do so, it is needed to increase the signal-to-noise ratio (SNR) of the system, especially when measuring in the far end of the fiber. In the past few years several techniques have been applied trying to achieve such goal¹⁻³. One widespread solution is the use of Raman assistance, either using first-order pumping⁴ or second-order pumping⁵. Raman amplification renders a distributed gain along the fiber that allows to partially compensate the inherent fiber losses. Despite the several advantages Raman assistance provides, it also brings Relative Intensity Noise (RIN) to the detected signal, mostly if Raman Fiber Lasers (RFL) are utilized as pumps.

In this paper, we show that Balanced Detection (BD) can be advantageously used in improving the SNR of BOTDA sensors. In particular, we demonstrate a general improvement of at least $\sqrt{2}$ in SNR and a complete cancellation of common-mode noise in the probe⁶. This last feature is extremely interesting for long-range Raman-assisted BOTDAs, where RIN transfer from the Raman pumps to the probe wave is a key concern. We show that with this type of detection, the RIN transfer problem can be completely avoided, thus unlocking the full potential of this technique.

2. PRINCIPLES

In order to apply BD to BOTDA systems, the probe signal is modulated with an amplitude modulator to obtain two symmetric sidebands at $\pm\nu_B$ with respect to the pump pulse frequency. Thus, stimulated Brillouin scattering (SBS) will amplify the lower frequency sideband and attenuate the higher frequency one. In detection, the sidebands are spectrally separated and fed into each detector of the BD. In typical conditions (when an external Mach-Zehnder electro-optic modulator is employed) the power of both the Stokes and Anti-Stokes bands is the same, and thus, the detected trace signal is naturally doubled in comparison with a single-detector scheme of equal responsivity⁶. Moreover, the DC component is rendered close to zero, and so the dynamic range of the detection system can be better exploited. The benefit of the technique is clear if we now turn our attention to the signal-to-noise ratio. In terms of noise, the summation of the two input noises coming from the two detectors (two independent equally-distributed random variables) will lead to an increase of $\sqrt{2}$ in noise. As the trace signal is doubled, the overall result is an increase of SNR of $\sqrt{2}$. Another interesting feature of this scheme is that any perturbation affecting both bands equally (common-mode noise) will be effectively cancelled by applying BD. Focusing on the particular scope of this paper, the RIN produced by the Raman pumping, will be equally found both in the Brillouin Gain (Stokes) and Brillouin Loss (Anti-Stokes) bands, and therefore will be eliminated upon detection.

*alejandrodominguezl@uah.es

3. EXPERIMENTAL SETUP

To prove the above analysis, we developed the BOTDA scheme represented in Fig. 1. It is a modification of the classical BOTDA system⁷ where the detection scheme has been modified to include balanced detection.

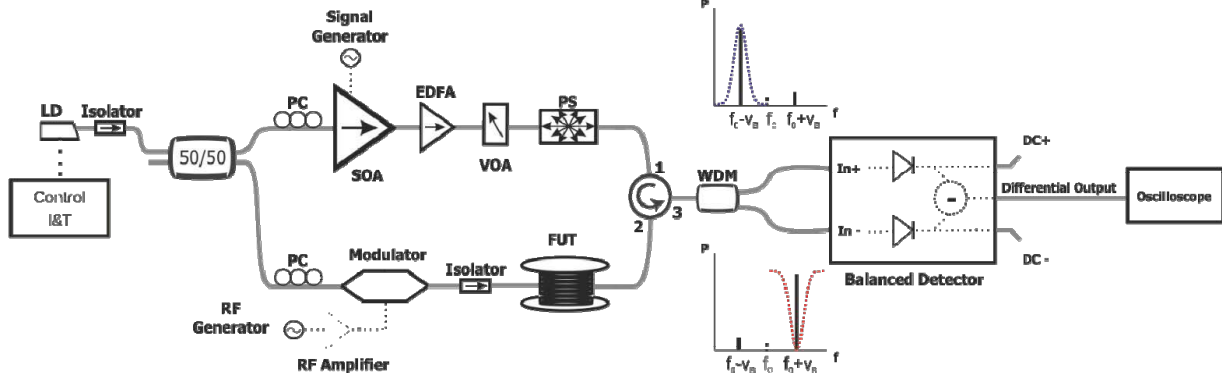


Fig. 1. Experimental setup of the BOTDA with Balanced Detection. LD: Laser Diode; PC: Polarization controller; EDFA: Erbium Doped Fiber Amplifier; RF: Radio-frequency generator; VOA: Variable Optical Attenuator; PS: Polarization Scrambler; WDM: Wavelength Division Multiplexer.

As in most BOTDA setups, pump and probe waves are developed from a single distributed feed-back (DFB) laser diode. The pump wave is pulsed using a Semiconductor Optical Amplifier (SOA), providing high extinction ratio (>30 dB) optical pulses. After pulsing, the optical signal is again amplified through an Erbium Doped Fiber Amplifier (EDFA). The power of the pulses is controlled through a Variable Optical Attenuator (VOA) and the polarization is scrambled by a fast polarization scrambler (5 MHz of scrambling rate). The pulse widths used are 40 ns (which implies the sensor has 4 meter resolution), and the pulse peak power provided is ~25 mW.

At the probe side, a Mach-Zehnder Electro-Optic Modulator (EOM) is used to make a dual sideband with suppressed carrier (DSB-SC) modulation. The probe power fed into the fiber is ~330 μ W on each sideband. The modulating frequency of the EOM is controlled through an RF Generator, which is swept around the Brillouin Frequency Shift (BFS) of the fiber under test. After going through the fiber and experiencing Brillouin Scattering, the probe sidebands are split using a DWDM filter, which separates the lower (gain) and higher (loss) probe frequencies. The attenuation of the rejected band is >13 dB in both cases. These two different bands are then fed to the positive and negative ports of the BD system. Ultimately, the BD System provides three different output signals: the Differential Output (with the signal of interest), and two monitoring outputs, where we read the DC levels of each of the input signals.

4. RESULTS

4.1 General advantages

We start by comparing measurements obtained with the same scheme using the gain band only (Gain-only measurements), the loss band only (Loss-only measurements), and finally the BD with both gain and loss bands (Balanced measurements). The measurements are performed over ~50 km of single mode fiber (SMF) with an essentially homogeneous BFS located at 10.883 GHz at the pump wavelength (~1550 nm).

The first remarkable result is that when acquiring in balanced mode, the trace amplitude of the Differential Output is twice the amplitude of any of the single sidebands, as illustrated in Fig.2a. Doubling the trace amplitude increases the signal contrast by 3 dB, which is potentially equivalent to 15 km of fiber. It also leads to a theoretical $\sqrt{2}$ SNR increase, as shown before. In addition, BD increases the robustness of the system to common-mode noises, which may affect both sidebands simultaneously (modulator drifts, master laser noise, RIN transfer, etc.) as we will see in Section 4.2. Fig. 2b also shows three gain profiles at a distance of 46.818 km, with a frequency sweep done from 10.82 GHz to 10.95 GHz. As it can be inferred, the noise of the differential output gain profile (bottom) is visibly reduced compared to the single sidebands cases (on top).

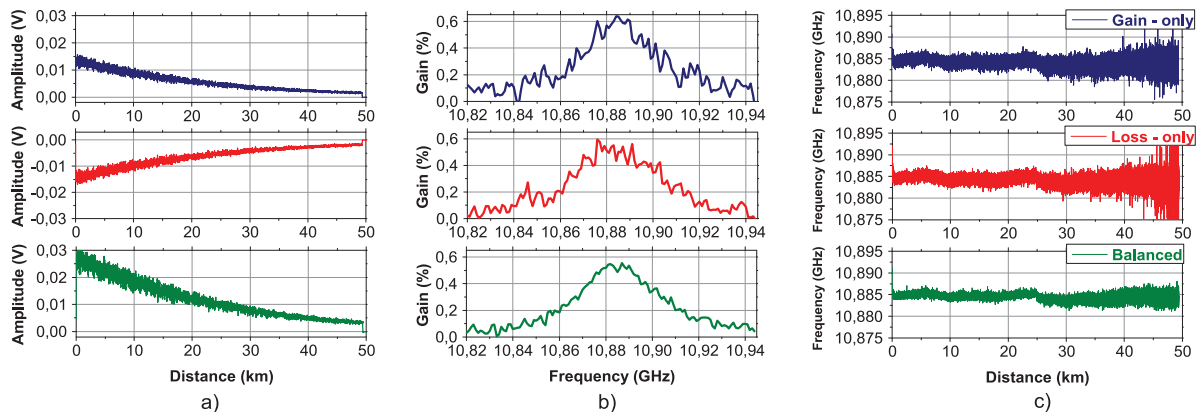


Fig. 2. Comparison of single sideband detection (top two) and BD (bottom). a) Trace obtained for a pump-probe frequency shift of 10.883 GHz. b) Gain profiles at 46.818 km for a frequency sweep between 10.82 GHz and 10.95 GHz. c) BFS for ~ 50 km of SMF.

Once the frequency sweep is finished, the BFS is obtained by fitting a 2nd order polynomial curve to the raw gain profile, and then finding the position of the maximum of the curve. As shown in Fig. 2c, finding the BFS at any point of the fiber is more accurate when BD is employed. The standard deviation of the obtained BFS between five consecutive traces is always $\sim\sqrt{2}$ lower in the balanced case, both at the beginning and at the end of the fiber. For any of the single sideband acquisitions, the fitting and finding the maximum processes might lead to points with extreme error, which are often observed at the end of the fiber. This situation is caused by the appearance of extreme peaks in the gain profile at that position, which perturb the fitting process. As it can be seen, the misleading points in the fitting and finding the maximum procedure are substantially avoided in the balanced case, even using raw gain profiles⁶.

4.2 RIN cancellation in first-order Raman assisted BOTDA

Since the first reports on Raman assistance in a BOTDA, RIN transfer has always been a major concern. Used in a Raman-assisted BOTDA, BD should provide complete cancellation of the RIN transfer issue. To prove this, we have introduced several modifications into the scheme presented in Fig. 1 in order to add first-order Raman amplification, allowing us to extend the measuring range up to ~ 100 km, analogous to a previous work from this group⁷. We used bi-directional Raman amplification pumped by a Raman Fiber Laser (RFL) emitting at 1455 nm. The RFL was coupled on each side by the use of suitable wavelength division multiplexers (WDMs). We performed all the measurements over ~ 100 km of SMF with an essentially homogeneous BFS located at 10.865 GHz at the pump wavelength (~ 1550 nm).

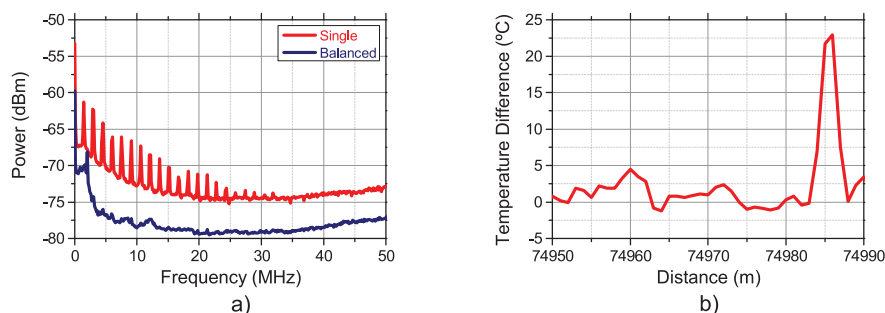


Fig. 3. a) Electrical spectra of the detected probe wave recorded for a total Raman pump power of ~ 360 mW. b) Brillouin frequency shift translated to temperature difference around a ~ 2 -meter hot-spot (located around km 75).

The most remarkable result is that, when acquiring in balanced mode, we accomplished an effective cancellation of the RFL RIN transfer. To evidence this, we performed electrical spectrum measurements of the intensity noise measured in detection, either using conventional (single-sideband) or BD. Fig. 3a shows the electrical spectra of the detected probe wave acquired in both detection setups, for a total Raman pump power of 360 mW (180 mW per each side). In single-sideband acquisition, the RIN transfer is well visible as a set of peaks with a periodic spacing of ~ 1.5 MHz. This frequency is given by the inverse of the cavity round-trip time of the primary Yb oscillator in the RFL pump. As it is

visible, these RIN noise peaks are completely eliminated in the BD case. This is an expected result due to the fact that the RIN is common to both the Brillouin Gain (Stokes) and Brillouin Loss (anti-Stokes) bands.

In order to achieve a proper cancellation of the RFL RIN, it is necessary to accurately match the optical path lengths of both Brillouin Gain and Loss bands. Small mismatch in the lengths will cause imperfect cancellation of the RIN especially at high frequencies. Nevertheless, high-frequency noise turns out to be more easily cancelled out in the conventional averaging procedure that is usually done in BOTDA. Hence we can safely affirm that most of the RIN transfer issues can be completely avoided by using this configuration.

To accomplish complete BOTDA measurements, a frequency sweep is done from 10.75 GHz to 10.95 GHz. In this case, the pulse width is reduced to 20 ns, leading to ~ 2 meter resolution measurements. The BFS is obtained in the same way as explained in Section 4.1. For each frequency step, only 1024 averages are carried out. The performance of the setup as a sensor was verified by placing a hot-spot in the position of worst contrast of the fiber (around km 75). This is done by immersing ~ 2 meters of fiber in a hot water bath. Again, a full frequency sweep is performed to retrieve the BFS change in the position of the hot-spot. The results of temperature change around the hot-spot are visible in Fig. 3b. The process of translating frequency to temperature difference is rather straightforward due to the fact that the relation temperature-frequency is linear (~ 1 °C/MHz). A ~ 22 °C elevation over room temperature was recorded in the hot-spot location. The system performs properly as a temperature sensor, as the temperature elevation is correctly verified with an external thermometer. The sensing uncertainty (estimated as the standard deviation of the repeatability) around the hot-spot (1000 m window) was ± 2 °C. The hot spot is also correctly identified as being ~ 2 -meter wide.

5. CONCLUSIONS

In conclusion, we have presented the application of a well-known detection technique (balanced detection) to BOTDA systems. This detection technique has several advantages when used in a BOTDA: the trace amplitude is doubled, the SNR is improved by at least a factor of $\sqrt{2}$, and the system shows strong robustness to common-mode noises (noises affecting equally both probe sidebands). With regards to the Raman-assisted configuration, this feature leads to a complete cancellation of the RIN transfer problem.

ACKNOWLEDGEMENTS

This work was supported in part by the European Research Council through U-FINE under Grant 307441, in part by the Spanish Ministry of Science and Innovation under Projects TEC2009-14423-C02-01 and TEC2009-14423-C02-02, the INTERREG SUDOE program ECOAL-MGT and in part by the Comunidad de Madrid under Project FACTOTEM-2. The work of S. Martín-López was supported by the Spanish Ministry of Science and Innovation through a “Ramón y Cajal” Contract.

REFERENCES

- [1] Angulo-Vinuesa, X., Martín-López, S., Nuno, J., Corredera, P., Ania-Castanon, J. D., Thevenaz, L. and Gonzalez-Herraez, M. “Raman-assisted Brillouin distributed temperature sensor over 100 km featuring 2 m resolution and 1.2° C uncertainty,” *IEEE J. Lightwave Technol.* 30(8), 1060-1065 (2012).
- [2] Soto, M. A., Sahu, P.K., Bolognini, G. and Di Pasquale, F. “Brillouin-based distributed temperature sensor employing Pulse Coding,” *IEEE Sensors J.* 8(3), 225–226 (2008).
- [3] Soto, M. A., Taki, M., Bolognini, G. and Di Pasquale, F. “Simplex-coded BOTDA sensor over 120-km SMF with 1-m spatial resolution assisted by optimized bidirectional Raman amplification,” *IEEE Photonic. Tech. Lett.* 24(20), 1823–1826 (2012).
- [4] Rodríguez-Barrios, F., Martín-López, S., Carrasco-Sanz, A., Corredera, P., Ania-Castañón, J.D., Thévenaz, L. and Gonzalez-Herraez, M. “Distributed Brillouin Fiber Sensor Assisted by First-order Raman Amplification,” *J. Lightwave Technol.* 28(15), 2162-2172 (2010).
- [5] Martín-López, S., Alcon-Camas, M., Rodríguez-Barrios, F., Corredera, P., Ania-Castañón, J.D., Thévenaz, L. and Gonzalez-Herraez, M. “Brillouin optical time-domain analysis assisted by second-order Raman amplification,” *Opt. Express* 18(18), 18769-18778 (2010).
- [6] Domínguez-López, A., López-Gil, A., Martín-López, S. and Gonzalez-Herraez, M. “Signal-to-noise ratio improvement in BOTDA using balanced detection”, *IEEE Photonic. Tech. Lett.* Accepted (2013).
- [7] Angulo-Vinuesa, X., Martín-López, S., Corredera, P. and Gonzalez-Herraez, M. “Raman-assisted Brillouin optical time-domain analysis with sub-meter resolution over 100 km,” *Opt. Express* 20(11), 12147-12154 (2012).